*Physicochem. Probl. Miner. Process., 58(6), 2022, 151692*

http://www.journalssystem.com/ppmp

Physicochemical Problems of Mineral Processing

ISSN 1643-1049


# Effective separation of specularite and aegirite using chitosan as a novel depressant

**Mingyang Li [1,2,3], Pengpeng Zhang [3], Xiangpeng Gao [3], Xiong Tong [1], Xian Xie [1]**

[1] Faculty of Land Resource Engineering, Kunming University of Science and Technology, Kunming 650093, China

[2] State Key Laboratory of Complex Nonferrous Metal Resources Clean Utilization, Kunming 650093, China

[3] School of Metallurgical Engineering, Anhui University of Technology, Ma'anshan 243002, China

Corresponding authors: kgxiongtong@163.com (X. Tong), kgxianxie@126.com (X. Xie)

**Abstract:** As a typical iron-bearing silicate gangue, aegirite often associates with specularite. Due to the iron element contained in aegirite, it has similar surface properties to specularite. Flotation is by far one of the most efficient methods of processing this kind of iron ore. But the traditional depressants unable to take action in the separation of specularite and aegirite. Chitosan was used as a novel depressant to attempt to separate specularite from aegirite through microflotation tests, adsorption tests, contact angle measurements, Zeta potential measurements, and XPS analysis. The flotation results indicate that chitosan show more strong depression effect on specularite than aegirite. Zeta potential measurements, contact angle measurements and adsorption tests demonstrate that chitosan is more inclined to adsorb on the specularite surface than aegirite, which hinders the subsequent adsorption of collector sodium oleate and increases difference in hydrophobicity between the two minerals. The XPS results of specularite validate the adsorption of chitosan on specularite, and illustrate that electrons of chitosan were partially transferred to oxygen and iron atoms in specularite during the adsorption process.

***Keywords:*** flotation, iron-bearing silicates, aegirite, specularite, chitosan, depressant

## 1. Introduction

Iron ore is an essential raw material for iron and steel making. With the increasing depletion of high-grade iron ore resources, the development and utilization of low-grade specularite ore resources and the recycling of abandoned low-grade specularite ore tailings have important practical significance (Pereira et al., 2021; Wang et al., 2021; Hao et al., 2018). According to the type of gangue, iron ore can be classified into quartz-type iron ore and silicate-type iron ore, among which silicate-type iron ore is more difficult to handle than quartz-type iron ore (Nakhaei et al., 2018; Al-Dhubaibi et al., 2019; Liu et al., 2020).

Iron ore mineral separation techniques are constantly challenged with the emergence of complex gangue minerals for iron-bearing silicate mineral, such as amphiboles, aegirite, pyroxenes, chlorite and others. In general, magnetic separation can achieve good results for many richer iron ores, but it cannot be guaranteed for such complicated ores. At present, the reverse flotation desiliconization process is mostly studied in the flotation separation of iron ore (Yao et al., 2016; Shrimali, 2016; Poperechnikova et al., 2017; Luo et al., 2016). Although this process has many advantages and is widely used, the conventional reverse flotation depressant starch inhibits aegirite in the same time, because aegirite can form strong chemical complexes with starch molecules (Veloso et al., 2018; Li et al., 2019; Li et al., 2020; Huang et al., 2012). In order to improve the effect of flotation separation of iron-containing silicate-type iron ore, many scholars have carried out research on novel flotation reagents, especially depressants. Veloso (Veloso et al., 2019) studied the depression effect of corn starch, dextrin, carboxymethyl cellulose (CMC) and humic acid, respectively, on the separation of iron ore containing berthierine and chamosite. The results indicate that high-molecular-weight CMCs are more likely to adsorb on the surface of the silicates leading to an increase in the silica content of the

DOI: 10.37190/ppmp/151692

final product, and that the carboxylic group of CMC preferentially adsorbs on the surface of minerals composed by metallic cations as $Ca^{2+}$, $Mg^{2+}$ and $Al^{3+}$.

Aegirite is a typical single-chain iron-bearing silicate mineral, which has similar surface properties and flotation characteristics to iron oxide ore as a result of the presence of element Fe in the crystal lattice (Li et al., 2019; Xu et al., 2016).As a result, during the reverse flotation separation process, the aegirite is easily mixed into the concentrate, which affects the separation effect.

Chitosan (CTS), as shown in Fig.1, is the product of the natural polysaccharide chitin that removes part of its acetyl group (Rinaudo, 2006). Due to its many functions such as biodegradability, non-toxicity, and bacteriostatic, it is widely used in food additives, textiles, agriculture, environmental protection, and drug development (Kurniawati et al., 2014; Desbrières & Guibal, 2018). In recent years, CTS and its derivatives have attracted more and more attention as a novel depressant. For example, Feng et al. (Feng et al., 2018a, 2018b; Qian et al, 2017) studied the selective inhibition effect of CTS on talc through experiments, and the inhibition of CTS on talc is mainly physical interaction. When the pH value is less than 9, because the amino protonated CTS is positively charged, the adsorption between CTS and talc surface is mainly carried out by hydrogen bonding. When the pH value was raised to about 9, in addition to the hydrogen bonds, non-selective deposits were formed on the surface of talc. Huang et al. (Huang et al., 2012) investigated the effect of two different degrees of deacetylation of CTS on the flotation separation of chalcopyrite and galena. The results showed that both the amide group and the protonated amine group of CTS were involved during the adsorption on chalcopyrite. While the adsorption of CTS on galena only involves amide groups, which results in poor inhibition effect, and the inhibition effect gradually decrease with the increase of the degree of deacetylation of CTS. The derivatives of CTS, for example, N-carboxymethyl CTS acts as a selective depressant of serpentine to promote the separation of serpentine and pyrite, and also as an effective depressant of calcite during calcite/apatite separation (Zhang et al., 2017). Dithiocarbamate chitosan (DTC-CTS) was also found to be a selective depressant for chalcopyrite in chalcopyrite/molybdenite flotation (Hao et al., 2022). However, no report on the application and mechanism of CTS in the separation of specularite and aegirite can be found.

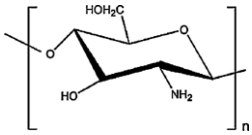


Fig. 1. Schematic diagram of molecular structure of CTS

In this work, the flotation separation of specularite ($Fe_2O_3$) and aegirite ($FeNaSi_2O_6$) using CTS as the depressant and sodium oleate as the collector was fully investigated. In addition, the CTS's depressant mechanism was researched via adsorption experiment, contact angle measurement and X-ray photoelectron spectroscopy.

## 2. Materials and methods

### 2.1. Materials

Aegirite and specularite were collected in Inner Mongolia and Anhui, China, respectively. To eliminate minor impurities, the high-grade lumps of ores were crushed and handpicked. The handpicked samples were further crushed and dry ground using a CGQM type agate mortar (Jilin exploration machinery plant, Changchun, China). Then the samples were sieved to different size fractions. The collector sodium oleate (NaOL), depressant CTS, pH modifiers HCl and NaOH were analytical-grade, and were all purchased from Adamas-beta® (Shanghai Titan Scientific Co. Ltd.). Deionized water with a resistivity of 18.2 MΩ·cm was utilized in all of the experiments.

### 2.2. Methods

#### 2.2.1. Characterization of materials

The compositions of aegirite and specularite samples were analyzed by ARL Advant'X Intellipow XRF analyzer (Thermo Fisher Scientific, USA). Prior to analysis, the materials were ground to a fineness of -

37 μm and compressed into solid discs. The two minerals were analyzed using X-ray diffraction in the 37 m size range by the D8 Advance X-ray powder diffractometer (Bruker Instruments Ltd., Germany).

### 2.2.2. Microflotation

The size fraction of aegirite and specularite samples between 37 μm and 74 μm were used for flotation. The proportion of aegirite and specularite in the mixed sample is 1:1, and the sample's total mass is 2 g. For a typical flotation experiment, 2 g sample was added into a flotation cell containing 40 mL deionized water. Then it was carried out in the following sequence: 1 min for pulp adjustment, 3 min for pH adjustment, 3 min for depressant reaction, 2 min for collector reaction, and 5 min for flotation. For single mineral flotation experiments, both the concentrate and tailings were collected, dried, and weighed to calculate the recovery. For the artificial mixed mineral flotation tests, the grade of Fe in products was assayed to calculate the separation efficiency.

### 2.2.3. Zeta potential measurements

Zeta potential measurements were conducted in a ZetaPALS potential analyzer (Brookhaven Instruments Ltd. US.). For a typical test, 5 mg of mineral sample (< 2 μm) was put into 50 mL 15 mg/L CTS solution with $1\times10^{-3}$ mol/L KCl as the background electrolyte solution under stirring, then the pH of each sample solution was adjusted to the required value and maintained for 2 min to be homogenized. After that, the Zeta potential was measured, and the results with the average values of three independent measurements were recorded.

### 2.2.4. Adsorption experiment

CTS concentration was measured according to the content of total organic carbon (TOC) by TOC-L (Shimadzu Japan). The residual concentration method was used to determine the quantity of CTS adsorbed on the mineral surface.

For a typical adsorption test, 2 g specularite or aegirite was dispersed uniformly in CTS solution at pH 8 for 1 h. After that, the content of TOC was measured for the supernatant generated by centrifugation. The quantity of CTS adsorption on minerals was determined using the following equation:

$$T = \frac{(C_0 - C_1)\times V}{m} \quad (1)$$

where $T$ (mg/g) was the CTS adsorption amount of mineral, $C_0$ and $C_1$(mg/L) represented the concentration of CTS before and after adsorption, respectively, $m$ (g) denoted the weight of mineral.

### 2.2.5. Contact angle measurement

Contact angle measurements were carried out using a JC2000A contact angle analyzer (Powereach Instruments, Shanghai, China). High-grade lumpish of aegirite and specularite were trimmed to a proper size, polished using polishing paper, and rinsed three times by deionized water. Then immersed the sample into the NaOL (60 mg/L) or CTS (15 mg/L) solution for 30 min and vacuum-dried at 40°C. 3.0 μL of deionized water droplet was dropped on the mineral surface via an automatic sample injection syringe before measuring the contact angle by capturing images of the water droplet profile using a computer. Each experiment was repeated five times, and the final outcome was based on the average value. .

### 2.2.6. XPS analysis

X-ray photoelectron spectroscopy (XPS) was conducted in a Thermo ESCALAB 250XI X-ray photoelectron spectrometer (Thermo Fisher Scientific, USA) with monochromatic Al Kα radiation as excitation source (pass energy 100 eV, energy step size 1 eV). Both survey and high-resolution spectra of O 1s, C 1s, N 1s and Fe 2p were recorded and calibrated to the binding energy of C 1s at 284.6 eV. In the case of XPS measurements, 1 g of specularite or aegirite with size fraction less than 2 μm was put into 100 mL CTS solution (15 mg/L) at pH 8. Then the modified suspension was filtered and dried

under vacuum at 25℃ for 24 h after being shaken for 1 h. The experiments were carried out after pressing the dried samples on a double side conductive adhesive carbon tape.

## 3. Results and discussion

### 3.1. Identification of minerals

The chemical composition of aegirite and specularite was listed in table 1. Aegirite sample was mainly composed of metal silicates with silicon, iron, sodium, calcium, aluminum, and magnesium silicates contributed to 91.7% of the total mineral. Specularite sample has shown a high purity where iron oxide consisted 95.74% of the total weight.

XRD patterns of aegirite and specularite were illustrated in Fig. 2. It can be seen from the results in Fig. 2 that only aegirite and specularite were identified in their respective diffraction pattern, which demonstrated their high purity. Combined with the results of chemical composition and XRD, the purity of the mineral samples met the requirements of various subsequent experiments.

Table 1. Chemical composition of aegirite and specularite

| Sample | Chemical composition content (%) | | | | | | |
|---|---|---|---|---|---|---|---|
| | $Fe_2O_3$ | $SiO_2$ | $Al_2O_3$ | MgO | $TiO_2$ | CaO | $Na_2O$ |
| Aegirite | 27.90 | 48.21 | 0.69 | 0.24 | - | 2.42 | 12.24 |
| Specularite | 95.74 | 3.36 | 0.38 | 0.23 | 0.08 | 0.04 | - |

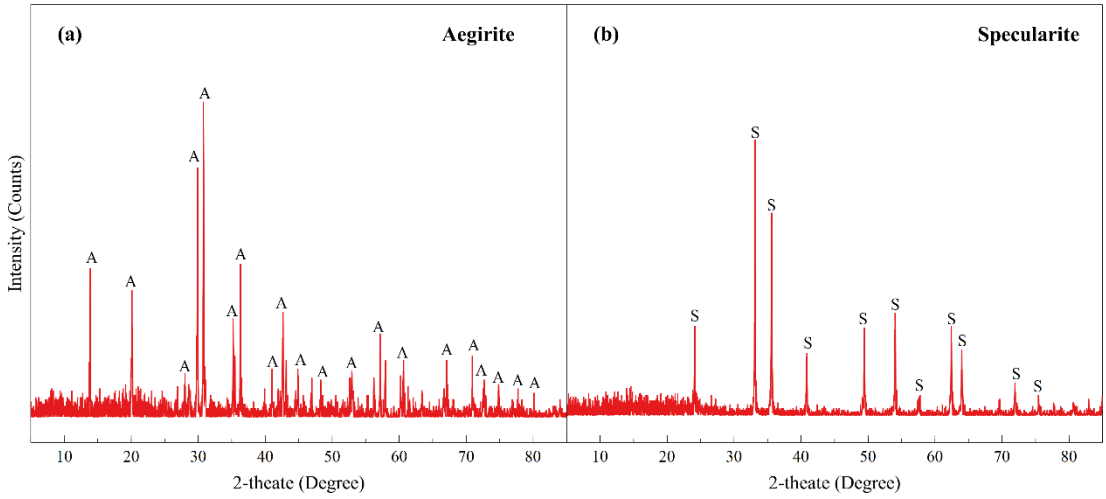


Fig. 2. XRD patterns of aegirite (a) and specularite (b) pure minerals

### 3.2. Flotation results

Fig. 3 presented the floatability of aegirite and specularite at different pH values and NaOL concentration, respectively. The concentration of NaOL was fixed at 40 mg/L in the first experiment. As shown in Fig. 3(a), the recoveries of two minerals were highly dependent on pH values, with optimum recoveries of 64.11% and 66.50% for aegirite and specularite at pH 6, respectively. Therefore, the optimum flotation pH was chosen at pH 6 and used in subsequent tests. The concentration of collector was varied from 20-100 mg/L to find the desirable recovery for specularite. Recoveries of both aegirite and specularite increases with the increasing NaOL concentration, with 86.26 and 89.36% recoveries at 60 mg/L collector concentration. Both recoveries reached plateau when the collector concentration is higher than 60 mg/L, thus the optimum NaOL concentration was selected at 60 mg/L for further experiments.

As can be observed in Fig. 3(b), the recoveries of the two minerals were both high under optimum experimental conditions, which is not efficient in flotation separation of these two minerals. Therefore a selective depressant are urgently needed to alter the flotation performance to achieve efficient

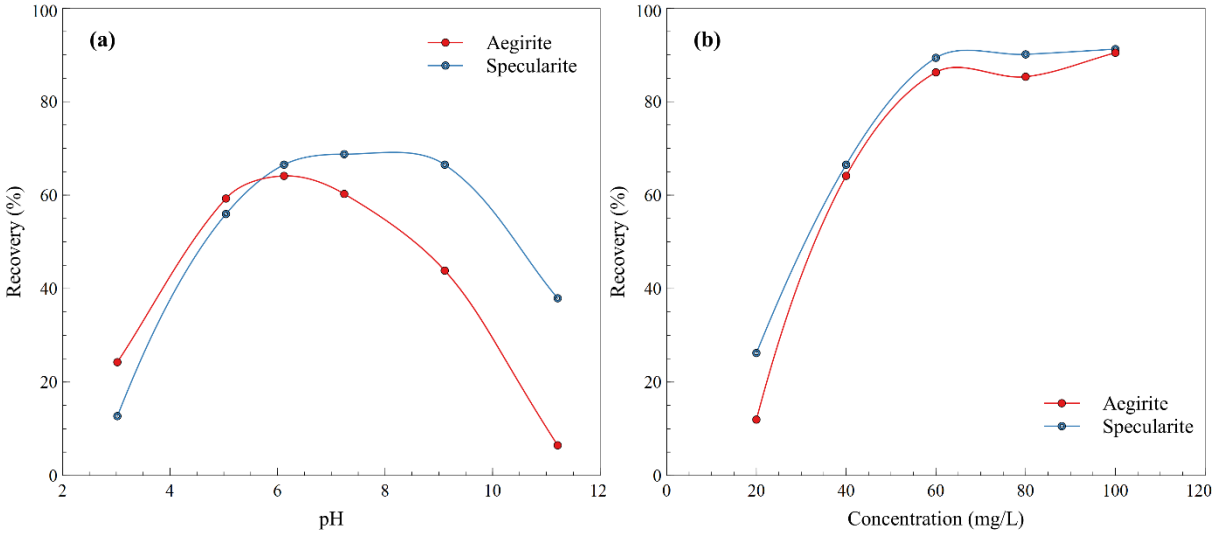


Fig. 3. Recovery of two minerals (a) as a function of pH with 40 mg/L NaOL and (b) as a function of NaOL concentration at pH 6

separation of aegirite and specularite. In this study, CTS was added into the flotation system as a selective depressant to separate specularite from aegirite. Fig. 4(a) illustrated the recoveries of two minerals with different CTS concentrations. CTS has exhibited a strong depress effect on specularite with the optimum separation of two minerals at 15 mg/L with recoveries of 56.83% and 8.73% for aegirite and specularite, respectively. Effect of pH on the depressing was examined with 15 mg/L CTS added as the depressant and shown in Fig. 4(b). CTS has presented good selective depressing effect on specularite in all pH ranges with largest recoveries different of two minerals at pH 8, where the recovery of specularite is 11.28% while 70.42% recovery of aegirite can be maintained. In single mineral flotation, CTS demonstrates exceptional selectivity and inhibition on specularite.

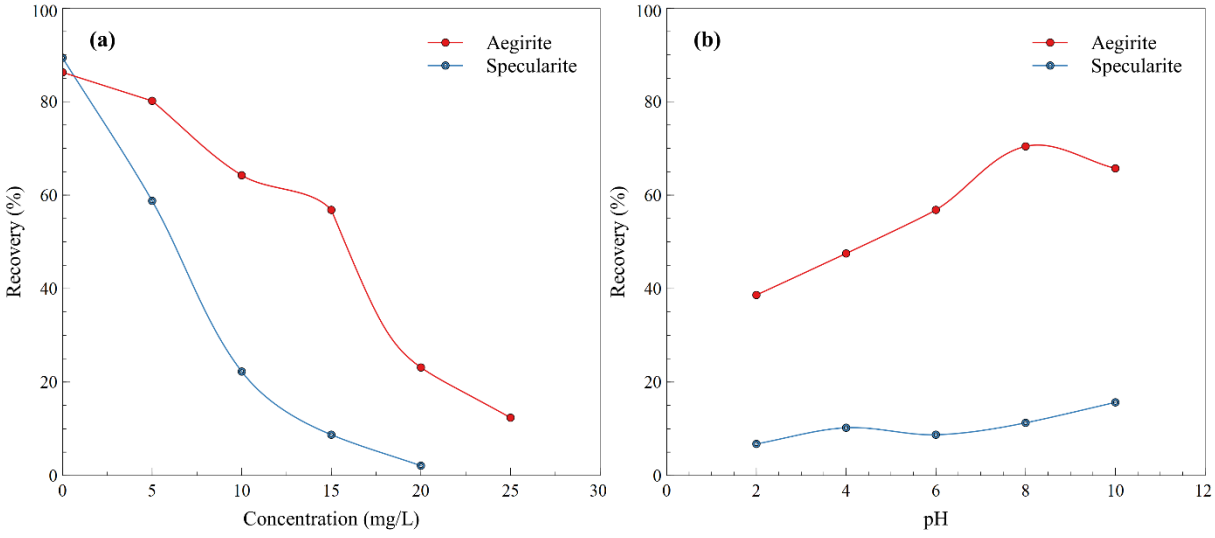


Fig. 4. Recovery of two minerals (a) as a function of CTS concentration at pH 6 and (b) as a function of pH with 15 mg/L CTS

Further flotation separation tests were conducted for aegirite and specularite mixed minerals at optimum experimental conditions with different CTS dosages and the results were presented in Table 2, and the relation of recovery-grade of the concentrate was shown in Fig. 4. The production and Fe recovery of concentrate increased with increasing CTS dosage, which suggested that CTS has inhibited the flotation properties of mixed minerals. However, the Fe grade reached maximum with CTS dosage at 15 mg/L, which is consistent with single mineral flotation results. Therefore, the

optimum depressant dosage is 15 mg/L, at which both Fe grade and recovery has significant improvement compared to direct flotation without depressant.

Table 2. Flotation separation of mixed mineral with different concentration of CTS

| The concentration of CTS (mg/L) | Products | Production (%) | Fe Grade (%) | Fe Recovery (%) |
|---|---|---|---|---|
| 0 | Concentrate | 26.24 | 47.63 | 28.69 |
| | Tailings | 73.76 | 42.11 | 71.31 |
| | Feeding | 100.00 | 43.56 | 100.00 |
| 5 | Concentrate | 39.47 | 51.83 | 47.52 |
| | Tailings | 60.53 | 37.32 | 52.48 |
| | Feeding | 100.00 | 43.05 | 100.00 |
| 10 | Concentrate | 46.74 | 54.72 | 59.13 |
| | Tailings | 53.26 | 33.19 | 40.87 |
| | Feeding | 100.00 | 43.25 | 100.00 |
| 15 | Concentrate | 49.62 | 56.48 | 65.28 |
| | Tailings | 50.38 | 29.58 | 34.72 |
| | Feeding | 100.00 | 42.93 | 100.00 |
| 20 | Concentrate | 54.15 | 54.22 | 67.77 |
| | Tailings | 45.85 | 30.45 | 32.23 |
| | Feeding | 100.00 | 43.32 | 100.00 |

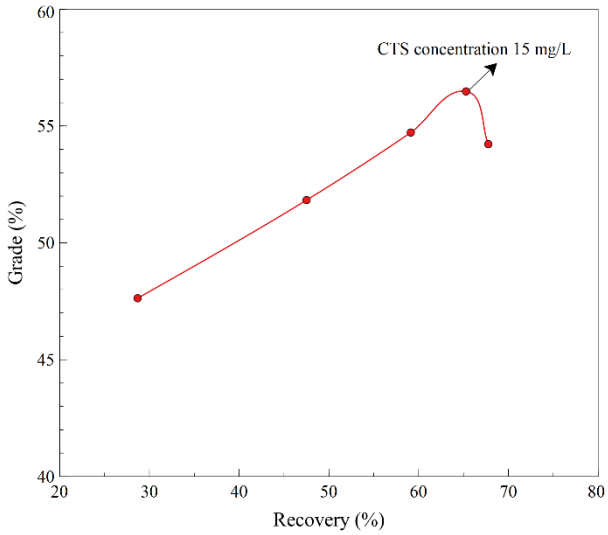


Fig. 5. The relation of recovery-grade of the concentrate

### 3.3. Zeta potential

Zeta potential of aegirite and specularite and the two minerals after CTS adsorption were recorded and illustrated in Fig. 5. Compared with these two minerals, the shift difference of zeta potential after CTS is discrepancy. In Fig. 5(a), zeta potential of aegirite has moved towards negative position under all pH values, and the shift at pH 6 is 13.78 mV. For specularite, the zeta potential change at pH 6 after CTS adsorption is 71.39 mV, which is significantly higher than aegirite and the surface charge has altered from positive to negative that resulted in the differential inhibition effect by CTS. This phenomenon suggested that CTS mainly adsorbed on specularite surface, and may generate chemically adsorb or hydrogen bonds on the mineral surface, which altered the surface charge on minerals thus further affected the adsorption of flotation collectors.

### 3.4. Adsorption measurements

The adsorption amount of CTS on the minerals increased with initial CTS concentration as indicated in Fig. 6. The amount of CTS adsorbed on specularite is obviously higher than that on aegirite, which

reflected that CTS has the selectively ability to attach to the surface of specularite. This conforms to the results of zeta potential and flotation, which also proved the changes of minerals surface properties after CTS inhibition.

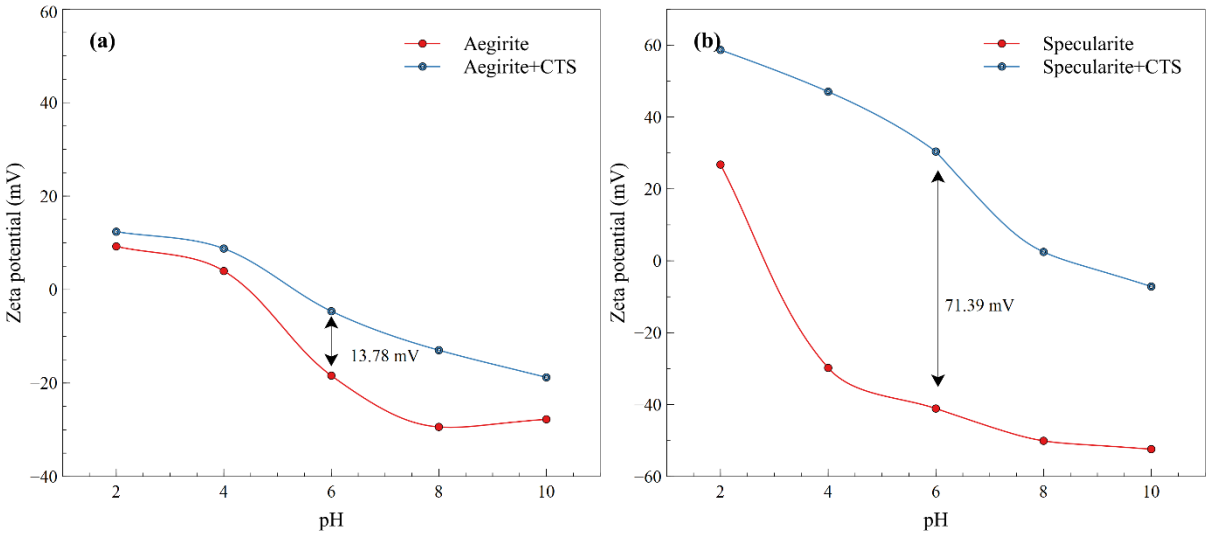


Fig. 6. The Zeta potential of (a) aegirite and (b) specularite treated by CTS

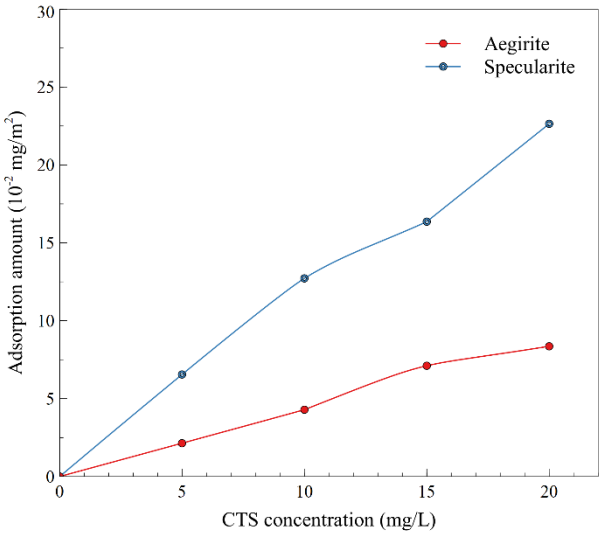


Fig. 7. The adsorption amount of CTS on aegirite and specularite with different concentration

### 3.5. Contact angle measurements

Contact angle is an important parameter representing the affinity of minerals toward flotation chemicals. We have examined the contact angles of aegirite and specularite, and these two minerals after reaction with NaOL and CTS. Table 3 shown that the contact angle aegirite and specularite was 43.3°and 50.4°, respectively, and that aegirite exhibited stronger hydrophilicity than specularite in aqueous solutions, which is consistent with the hypothesis and prior findings (Li et al., 2020). The contact angle of two minerals both increased after adsorbing NaOL, suggesting that NaOL has enhanced both hydrophilicities of minerals. However, CTS has completely altered the hydrophilicity with contact angles of 32.6° and 28.7°, respectively for aegirite and specularite. The addition of NaOL after CTS restored the contact angle of aegirite to 59.3°, while the contact angle of specularite did not change significantly. The results show that although the adsorption of CTS on both minerals occurs, the adsorption of CTS on aegirite does not hinder the subsequent adsorption of NaOL and does not reduce its floatability. This results in the selective inhibition of specularite by CTS during specularite/aegirite separation.

Table 3. Contact angle measurement results (pH=8; NaOL concentration: 60 mg/L; CTS 15 mg/L)

| Test system | Aegirite | Specularite |
|---|---|---|
| Without reagent | 43.3° | 50.4° |
| With NaOL | 64.8° | 67.3° |
| With CTS | 32.6° | 28.7° |
| With CTS+ NaOL | 59.3° | 34.9° |

### 3.6. XPS

XPS spectrum of specularite and specularite after CTS treatment were recorded to identify the surface interactions of specularite with functional groups. Full range scan of two samples was shown in Fig. 7, where Fe 2p, O 1s, C 1s, and Si 2p peaks can be observed on both samples and N 1s appeared after CTS treatment, which further proofs that CTS adsorb on the surface of specularite. Compared to specularite, there is no obvious changes of the aegirite XPS spectra with being treated by CTS, except the intensity decline of Na peak. The decline of Na peak intensity are mainly caused by the surface dissolution. The not obvious change in XPS spectra of aegirite after treating by CTS indicated that the adsorption of CTS on aegirite surface is poor.

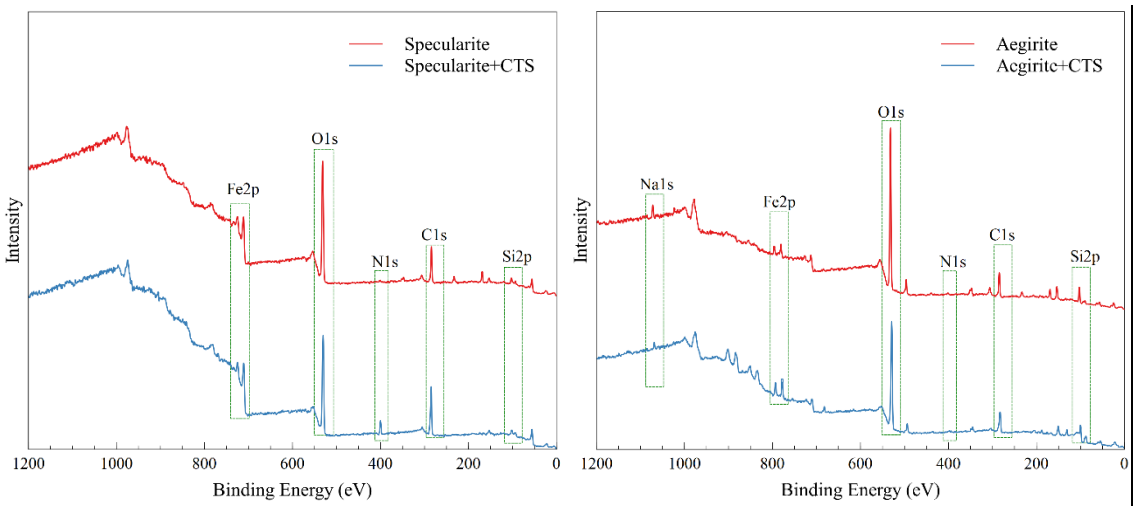


Fig. 8. XPS spectra of specularite and aegirite with and without being treated by CTS

High resolution XPS spectrum of C 1s, O 1s, N 1s, and Fe 2p with their deconvoluted fitting curves were presented in Fig 8. From Fig. 8(a) and (b), the intensities of C-O and C-N has increased after CTS adsorption, indicating the adsorption of CTS molecules on the mineral surface. Two deconvoluted fitting curves at 532.3 and 530.5 eV can be observed in O 1s spectra in Fig. 8(c), which were attributed to O-Si and O-Fe peaks, respectively. After CTS adsorption, these two peaks have shifted to lower binding energies, indicating that the oxygen atoms on the specularite were electron acceptors in the adsorption process (Wang et al., 2019). New peaks at 531.6 and 530.6 eV were also discovered in Fig. 8(d), which were corresponded to organic C-O and C-O-C bonds from CTS. Two characteristic peaks on amino and protonated amino at 397.2 and 398.7 eV were demonstrated in Fig. 8(f), suggesting the involvement of CTS polymer (Liu et al., 2020). Peaks of Fe 2p all shifted to significantly lower binding energies, which denoted that iron atoms dominated the adsorption process and accept shared electrons from CTS.

## 4. Conclusions

Using NaOL as a collector, the inhibitory effect and mechanism of CTS in the process of specularite/aegirite separation were studied. The main conclusions are as follows:

(1) The floatability of aegirite and specularite reached optimal value with 86.26% and 89.36%, respectively, when the concentration of NaOL was 60 mg/L; when CTS (15 mg/L) was used as

the inhibitor, aegirite and specularite were selectively inhibited, with the best recoveries of 70.42% and 11.28%, respectively.

(2) CTS can be adsorbed on both aegirite and specularite, but the adsorption amount on the specularite surface is significantly larger than that on aegirite, and the CTS adsorbed on the specularite surface can hinder the subsequent adsorption of NaOL.

(3) During the adsorption of specularite by CTS, Fe atoms on the surface of specularite received part of the electrons from CTS.

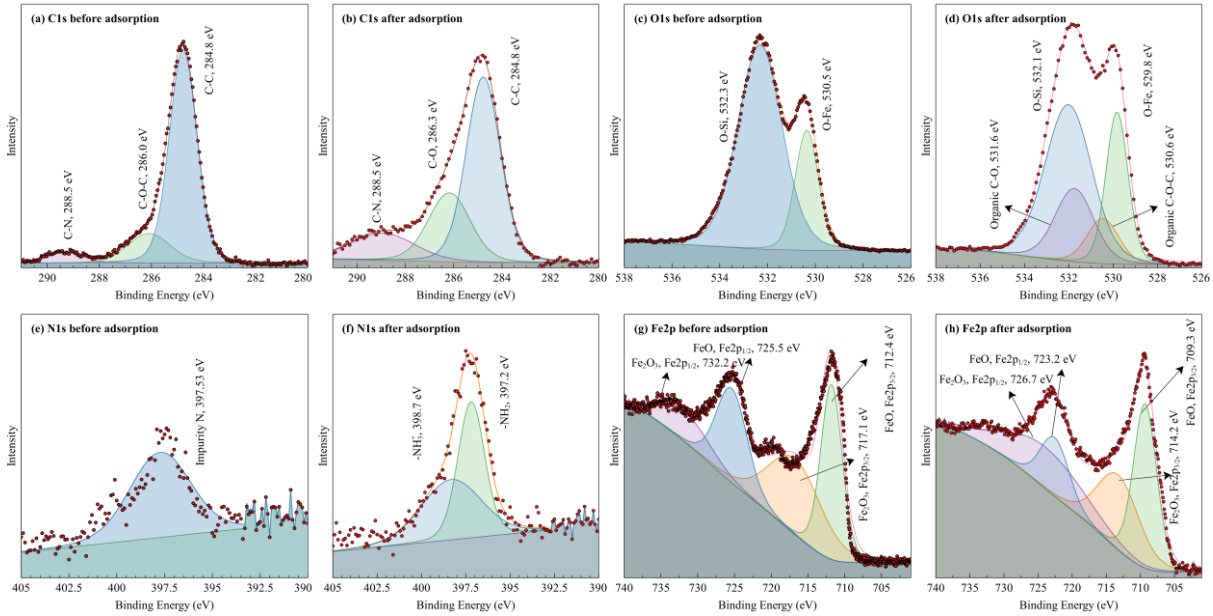


Fig. 9. High-resolution spectra of XPS on C1s, O1s, N1s, and Fe2p before and after CTS adsorption

## Acknowledgments

This work was supported by the financial support from the National Natural Science Foundation of China (51904001), China Postdoctoral Science Foundation funded project (2020M673590XB) and the Open Project Program of State Key Laboratory of Complex Nonferrous Metal Resources Clean Utilization (CNMRCUKF2202).

## References

AL-DHUBAIBI, A. M., VAPUR, H., SONER, T. O. P., 2019. *Effective processing of specularite ore by wet magnetic separation and reverse flotation techniques*. Hittite Journal of Science and Engineering, 6(3), 201-208.

DESBRIères, J., GUIBAL, E., 2018. *Chitosan for wastewater treatment*. Polymer International, 67(1), 7-14.

FENG, B., PENG, J., GUO, W., ZHU, X., HUANG, W., 2018. *The stimulus response of chitosan and its depression effect on talc flotation*. Mineral Processing and Extractive Metallurgy, 127(1), 56-61.

FENG, B., PENG, J., GUO, W., ZHANG, W., AI, G., WANG, H., 2018. *The effect of changes in pH on the depression of talc by chitosan and the associated mechanisms*. Powder Technology, 325, 58-63.

HAO, H., LI, L., YUAN, Z., LIU, J., 2018. *Comparative effects of sodium silicate and citric acid on the dispersion and flotation of carbonate-bearing iron ore*. Journal of Molecular Liquids, 271, 16-23.

HAO, J., LIU, J., YANG, D., QIN, X., GAO, H., BAI, X., WEN, S., 2022. *Application of a new depressant dithiocarbamate chitosan in separation of chalcopyrite and molybdenite*. Colloids and Surfaces A: Physicochemical and Engineering Aspects, 634, 127920.

HUANG, G., ZHOU, C., LIU, J., 2012. *Effects of different factors during the desilication of diaspore by direct flotation*. International Journal of Mining Science and Technology, 22(3), 341-344.

HUANG, P., CAO, M., LIU, Q., 2012. *Adsorption of chitosan on chalcopyrite and galena from aqueous suspensions*. Colloids and Surfaces A: Physicochemical and Engineering Aspects, 409, 167-175.

KURNIAWATI, H. A., ISMADJI, S., LIU, J. C., 2014. *Microalgae harvesting by flotation using natural saponin and chitosan*. Bioresource technology, 166, 429-434.

LI, M., LIU, J., GAO, X., HU, Y., TONG, X., ZHAO, F., YUAN, Q., 2019. *Surface properties and floatability comparison of aegirite and specularite by density functional theory study and experiment*. Minerals, 9(12), 782.

LI, M., LIU, J., HU, Y., GAO, X., YUAN, Q., ZHAO, F., 2020. *Investigation of the specularite/chlorite separation using chitosan as a novel depressant by direct flotation*. Carbohydrate polymers, 240, 116334.

LIU, J., EJTEMAEI, M., NGUYEN, A. V., WEN, S., ZENG, Y., 2020. *Surface chemistry of Pb-activated sphalerite*. Minerals Engineering, 145, 106058.

LIU, W., LIU, W., ZHAO, Q., PENG, X., WANG, B., ZHOU, S., ZHAO, L., 2020. *Investigating the performance of a novel polyamine derivative for separation of quartz and hematite based on theoretical prediction and experiment*. Separation and Purification Technology, 237, 116370.

LUO, X. M., YIN, W. Z., WANG, Y. F., SUN, C. Y., MA, Y. Q., LIU, J., 2016. *Effect and mechanism of siderite on reverse anionic flotation of quartz from hematite*. Journal of Central South University, 23(1), 52-58.

NAKHAEI, F., IRANNAJAD, M., 2018. *Reagents types in flotation of iron oxide minerals: A review*. Mineral Processing and Extractive Metallurgy Review, 39(2), 89-124.

PEREIRA, A. R. M., HACHA, R. R., TOREM, M. L., MERMA, A. G., SILVAS, F. P., 2021. *Direct hematite flotation from an iron ore tailing using an innovative biosurfactant*. Separation Science and Technology, 1-11.

POPERECHNIKOVA, O. Y., FILIPPOV, L. O., SHUMSKAYA, E. N., FILIPPOVA, I. V., 2017. *Intensification of the reverse cationic flotation of hematite ores with optimization of process and hydrodynamic parameters of flotation cell.* Journal of Physics: Conference Series, 879(1), 012016.

QIAN, G., BO, F., DANPING, Z., JUJIE, G., 2017. *Flotation separation of chalcopyrite from talc using carboxymethyl chitosan as depressant*. Physicochemical Problems of Mineral Processing, 53(2), 1255-1263.

RINAUDO, M., 2006. *Chitin and chitosan: Properties and applications*. Polymer Science, 31(7), 603–632.

SHRIMALI, K., MILLER, J. D., 2016. *Polysaccharide depressants for the reverse flotation of iron ore*. Transactions of the Indian Institute of Metals, 69(1), 83-95.

VELOSO, C. H., FILIPPOV, L. O., FILIPPOVA, I. V., & ARAUJO, A. C., 2019. *The effect of pH on the depression of iron oxides in the presence of complex gangue silicate minerals*. IMPC 2018-29th International Mineral Processing Congress, 1718-1723.

VELOSO, C. H., FILIPPOV, L. O., FILIPPOVA, I. V., OUVRARD, S., ARAUJO, A. C., 2018. *Investigation of the interaction mechanism of depressants in the reverse cationic flotation of complex iron ores*. Minerals Engineering, 125, 133-139.

WANG, X., LIU, W., DUAN, H., LIU, W., SHEN, Y., GU, X., QIU, J., JIA, C., 2021. *Potential application of an eco-friendly amine oxide collector in flotation separation of quartz from hematite*. Separation and Purification Technology, 278, 119668.

WANG, Y., AHMED KHOSO, S., LUO, X., TIAN, M., 2019. *Understanding the depression mechanism of citric acid in sodium oleate flotation of $Ca^{2+}$-activated quartz: Experimental and DFT study*. Minerals Engineering, 140, 105878.

XU, L., HU, Y., WU, H., TIAN, J., LIU, J., GAO, Z., WANG, L., 2016. *Surface crystal chemistry of spodumene with different size fractions and implications for flotation. Separation and Purification* Technology, 169, 33-42.

YAO, J., YIN, W., GONG, E., 2016. *Depressing effect of fine hydrophilic particles on magnesite reverse flotation*. International Journal of Mineral Processing, 149, 84-93.

ZHANG, C., LIU, C., FENG, Q., CHEN, Y., 2017. *Utilization of N-carboxymethyl chitosan as selective depressants for serpentine on the flotation of pyrite*. International Journal of Mineral Processing, 163, 45-47.